MONOGRAPHS ON THE PHYSICS AND CHEMISTRY OF MATERIALS • 64

Introduction to Scanning Tunneling Microscopy

Second Edition

C. JULIAN CHEN

OXFORD SCIENCE PUBLICATIONS

The scanning tunneling microscope and the atomic force microscope, both capable of imaging and manipulating individual atoms, were crowned with the Nobel Prize in Physics in 1986, and are the cornerstones of nanotechnology today.

The second edition of this book includes a number of new developments in the field. A chapter about the underlying physics of non-contact atomic-force microscopy has been added, the chapter on atomic force microscopy has been substantially expanded, and a pedagogical presentation of the basic concepts of spin-polarized STM is now included. The underlying theory and new instrumentation for inelastic scanning tunneling microscopy are added, as are advances in the field of biological research, emphasising the increase of the speed of scanning to observe life phenomena in real time. The capability of STM to manipulate individual atoms is one of the key developments of nanotechnology. The theoretical basis and in particular the relation between tunneling and interaction energy are thoroughly presented in this book, together with experimental facts.

C. Julian Chen is Adjunct Senior Research Scientist and Adjunct Professor at the Department of Applied Physics and Applied Mathematics, Columbia University.

Praise for *Introduction to Scanning Tunneling Microscopy*:

'Provides a good introduction to the field for newcomers and also contains valuable material and hints for experts.' H. Rohrer, IBM, Nobel Prize winner 1986

'. . . Will become a 'bible' for STM students.'
John Pethica, University of Oxford, UK

'An excellent book . . . Suitable for use as a textbook in the senior undergraduate and graduate levels, as well as a reference book for students and professionals.'
D. D. L. Chung, SUNY Buffalo, Journal of Minerals, Metals and Materials Society

'It will be of great use to the scientific community, particularly for new researchers getting started in the field of STM . . . The theoretical section is extremely comprehensive . . . The chapters on instrumentation are excellent.'
Shirley Chiang, IBM

'A remarkable achievement . . . A beautiful piece of work.'
Andrew Briggs, University of Oxford, UK

'It is an excellent book which will benefit students and scientists alike.'
Tien T. Tsong, Pennsylvania State University, USA

OXFORD
UNIVERSITY PRESS

www.oup.com

ISBN 978-0-19-875475-6
9 780198 754756

Introduction to Scanning Tunneling Microscopy

Second Edition

C. Julian Chen

Department of Applied Physics and Applied Mathematics
Columbia University, New York

OXFORD

UNIVERSITY PRESS

MONOGRAPHS ON THE PHYSICS AND CHEMISTRY OF MATERIALS

Theory of dielectrics H. Frohlich
Strong solids (Third edition) A. Kelly and N. H. Macmillan
Optical spectroscopy of inorganic solids B. Henderson and G. F. Imbusch
Quantum theory of collective phenomena G. L. Sewell
Principles of dielectrics B. K. P. Scaife
Surface analytical techniques J. C. Rivière
Basic theory of surface states Sydney G. Davison and Maria Steslicka
Acoustic microscopy G. A. D. Briggs
Light scattering: principles and development W. Brown
Quasicrystals: a primer (Second edition) C. Janot
Interfaces in crystalline materials A. P. Sutton and R. W. Balluffi
Atom probe field ion microscopy M. K. Miller, A. Cerezo, M. G. Hetherington, and G. D. W. Smith
Rare-earth iron permanent magnets J. M. D. Coey
Statistical physics of fracture and breakdown in disordered systems B. K. Chakrabarti and L. G. Benguigui
Electronic processes in organic crystals and polymers (Second edition) M. Pope and C. E. Swenberg
NMR imaging of materials B. Blümich
Statistical mechanics of solids L. A. Girifalco
Experimental techniques in low-temperature physics (Fourth edition) G. K. White and P. J. Meeson
High-resolution electron microscopy (Third edition) J. C. H. Spence
High-energy electron diffraction and microscopy L.-M. Peng, S. L. Dudarev, and M. J. Whelan
The physics of lyotropic liquid crystals: phase transitions and structural properties A. M. Figueiredo Neto and S. Salinas
Instabilities and self-organization in materials, Volume 1: Fundamentals of nanoscience, Volume 2: Applications in materials design and nanotechnology N. Ghoniem and D. Walgraef
Introduction to scanning tunneling microscopy (Second edition) C. J. Chen

Preface to the Second Edition

In a 1959 speech entitled *There's Plenty of Room at the Bottom* [1], Richard Feynman invited scientists to a new field of research: to see individual atoms distinctly, and to arrange the atoms the way we want. Feynman envisioned that, by achieving those goals, one could synthesize any chemical substance that the chemist writes down, resolve many central and fundamental problems in biology at the molecular level, and dramatically increase the density of information storage. Some 20 years later, those goals began to be achieved through the invention and application of the scanning tunneling microscope (STM) [2, 3] and the atomic force microscope (AFM) [4]. The inventors of STM, two physicists at IBM Research Division, Gerd Binnig and Heinrich Rohrer, shared the 1986 Nobel Prize in physics [5, 6].

At that time, I was fortunate to be in the Department of Physical Sciences of IBM Research Division, and had the opportunity to design, build, and run those fascinating instruments. Partially based on my personal experience and understanding, in 1993, the first edition of this book was published [7]. In the decade following, Feynman's foresight has grown into a vast field of research, nanoscience and nanotechnology. As a result, tremendous advances have been achieved in the understanding of the basic physics as well as instrument design and operation of STM and AFM. It is time to publish a second edition to include those recent advances, and to satisfy the urgent need for an updated, unified, accurate, and pedagogically assessable textbook and reference book on STM and AFM.

During the years of 1994 to 2003, I was concentrating on the research of human voice and languages, which were my favorite subjects ever since my college years. And I received more corporate recognition than for my basic research in physics [8]. However, the news about the advancements in STM and AFM constantly called me to come back to nanoscience and nanotechnology. In December 2003, I received a kind invitation from Professor Roland Wiesendanger, the Director of the Institute of Applied Physics at Hamburg University, to become a guest scientist. This is one of the largest and most productive centers of STM and AFM research, especially in spin-polarized STM and non-contact AFM. And for the first time in my life, I could concentrate 100% of my time on nanoscience and nanotechnology research. In the summer semester of 2005, in a graduate-level course in nanostructure physics jointly given to the Department of Physics and the Department of Chemistry at Hamburg University, Professor Roland Wiesendanger lectured the analyses of various nanostructures, and I lectured the principles and instrumentation of STM and AFM. The lecture notes on STM and AFM then became the blueprint of the second edition of the STM book.

Following are some examples of the additions to the second edition:

Atomic force microscopy, with a refined frequency-modulation mode,

has achieved true atomic resolution in the *attractive atomic force regime*, often referred to as the *non-contact AFM*. In some cases, its resolution has even surpassed that of STM. The observed bias-dependence of atomic forces provides information about the details of electronic structure. This new technique enables atomic-scale imaging and characterization not only for conductors, but also for insulators.

Significant breakthrough in spin-polarized STM has enabled the observation of local magnetic phenomena down to atomic scale. Such advancement was to drive the development of nanomagnetism, which would have deep impact on the technological applications of magnetism.

Inelastic electron tunneling spectroscopy (IETS), initially discovered in metal-insulator-metal tunneling junctions to observe vibrational frequencies of embedded molecules, was advanced to STM junctions, enabling the observation of vibrational states of *individual molecules*. The successful demonstration of STM-IETS elevated the field of single-molecule chemistry to an unprecedented level.

At the time that the first edition was written, atom manipulation was still a highly specialized personal art. In the later years, the underlying physics has gradually been discovered, and the atom-manipulation process is becoming a precise science. Besides single atoms, molecules are also subject to manipulation. It was often said that STM is to nanotechnology what the telescope was to astronomy. Yet STM is capable of *manipulating* the objects it observes, to build nanoscale structures never existed in Nature. No telescope is capable of bringing Mars and Venus together.

In the process of further improving the resolution of STM and AFM, the understanding of its basic physics has been advanced. Numerous convincing theoretical and experimental studies have shown that the imaging mechanism of both STM and AFM at atomic resolution can be understood as a sequence of making and breaking of partial covalent bonds between the anisotropic quasi-atomic orbitals on the tip and those on the sample. The nature of STM and AFM, including those with spin-polarized tips, can be understood with a unified perspective based on Heisenberg's concept of *resonance* in quantum mechanics.

Commercialization of STM and AFM has been greatly advanced. Owing to the rapidly expanding research in nanotechnology, especially in molecular biology and in materials science, AFM with tapping mode operating in air or in liquid now constitutes the largest market share. Therefore, a brief presentation of its basic principles is included.

In spite of the availability of commercial STMs and AFMs, research groups worldwide continue to design and build customized instruments to achieve advanced features and to serve special experimental needs. Often, those new designs are then adapted by instrument manufacturers to become products. Although the basic principles of the design and construction of STM and AFM was laid down in the second part of the first edition,

Instrumentation, new trends and ideas have been added.

The basic organization of the second edition is essentially identical to the first edition. All the materials in the first edition proven to be useful are preserved. Some of the less important materials are eliminated or converted to Problems at the ends of various chapters. The first chapter, *Overview*, is preserved but updated. Several recent applications of STM and AFM, probably of interest to general readers, are added. The title of the first Part is changed to *Principles* from *Imaging Mechanism* because of the inclusion of the physics of *atom and molecule manipulation*. The *Gallery of STM Images* is updated, with more historical photos and AFM images added, which is now entitled simply *Gallery*. To preserve the classical style of the first edition and to reduce the cost of printing, all photographs and images are in black-and-white. Similar to the first edition, only a few illustrative applications of STM and AFM are presented, because there are already many excellent books on various applications. For example, the monograph *Scanning Probe Microscopy and Spectroscopy: Methods and Applications* by R. Wiesendanger [9]; the book series *Scanning Tunneling Microscopy* I, II, and III edited by R. Wiesendanger and H.-J. Güntherodt [10]; *Scanning Tunneling Microscopy* edited by J. A. Stroscio and W. J. Kaiser [11]; the second edition of the monograph *Scanning Tunneling Microscopy and its Applications* by C. Bai [12]; and the second edition of *Scanning Probe Microscopy and Spectroscopy: Theory, Techniques, and Applications* edited by D. Bonnell [13]. Similar to the first edition, to ensure pedagogical soundness, the focus is on simple but useful theories, with every derivation presented in full detail. Many new figures are added to illustrate the concepts in physics. In the second edition, care has been taken to use SI units as much as possible. That would provide a unified order-of-magnitude mental picture of the physical quantities involved. Because of the enormous growth of the size of literature, the reference list at the back of the second edition only includes those cited by the text, selected and arranged automatically by LaTeX. In the age of the Internet, exhaustive reference lists can be obtained by searching on the web.

The author is deeply grateful to H. Rohrer for commenting extensively on the manuscript of the first edition, and publicly recommending the book to newcomers as well as experts. The author is equally grateful to Ch. Gerber, an architect of both the first STMs and the first AFMs, for comments on the second edition, and especially for providing a number of precious original photographs and images of historical interest. An early manuscript of the second edition was thoroughly reviewed by a number of experts in that field. Corrections and improvements were made upon their comments. Following is an incomplete list. The entire book by K.-H. Rieder of Swiss Federal Laboratories for Materials Research. Part I and Chapter 15 by R. Pérez of Universidad Autonoma de Madrid. Part II, especially Chapter 15, by F. Giessibl of University of Regensburg. All chapters related to scanning

tunneling spectroscopy and spin-polarised STM by O. Pietzsch of Hamburg University. The main part of Chapter 1 and Chapter 12 by F. Besenbacher, J. V. Lauritsen, and E. Laegsgaard of University of Aarhus. Chapter 9 by W. Coburn and P. Stokes of EBL Products, Inc., and M. Ordillas of Morgan Electro Ceramics, Inc. Chapter 14 by R. Feenstra of Carnegie Melon University. Chapter 15, especially Section 15.4, by C. Prater of Veeco Instruments Inc. Section 1.5.2 and Section 13.6 by the group of J. Ulstrup of Technical University of Denmark. Section 1.5.4 by J. Hu of Jiaotong University, Shanghai. Section 13.3.5 by R. A. Wolkow of University of Alberta. Last but not least, Sections 5.2.1, 5.2.2, and 5.2.3 by W. Hofer of University of Liverpool.

The Gallery is an integrated part of the book. The author is indebted to the following authors who contributed high-resolution black-and-white original photographs and images for the publication of this book: Plates 2, 3, and 4, Ch. Gerber. Plate 5, R. Wiesendanger. Plates 7, 11, 12, and 16, J. Boland. Plates 8, 10, and 15, R. Feenstra. Plate 9, J. V. Barth. Plate 13, D. J. Thomson. Plate 14, J. Repp and G. Meyer. Plate 17, M. Bode. Plate 18, L. Berbil-Bautista. Plate 19, O. Pietzsch. Plate 20, A. R. Smith. Plates 21 and 22, S. Fölsch. Plate 23, K. F. Braun. Plates 24, P. Weiss. Plate 25, C. F. Hirjibehedin. Plate 27, F. J. Giessibl. Plate 28, J. V. Lauritsen and F. Besenbacher. Plate 29, R. Pérez and Ó. Custance. Plate 30, Ó. Custance.

C. Julian Chen

Columbia University
in the City of New York

July 2007

Gallery

Plate 1. The IBM Zurich Laboratory soccer team. On October 15, 1986, the soccer team of IBM Zurich Laboratory and Dow Chemical played a game which had been arranged earlier. To everyone's surprise, a few hours before the game, the Swedish academy announced the Nobel Prize for Gerd Binnig (right, holding flowers) and Heinrich Rohrer (left, holding flowers). Newspaper reporters rushed in for a press conference.

Towards the end of the press conference, Binnig and Rohrer said that they must leave immediately because both were members of the laboratory soccer team. The reporters followed them to the soccer field. A photographer for the Swiss newspaper Blick took this photograph before the game started. At the center of the photograph, holding a soccer ball is Christoph Gerber, responsible for building the first scanning tunneling microscope as well as the first atomic force microscope.

(Original photograph by courtesy of IBM Zurich Laboratory.)

Chapter 1
Overview

1.1 The scanning tunneling microscope

The scanning tunneling microscope (STM) was invented by Binnig and Rohrer and implemented by Binnig, Rohrer, Gerber, and Weibel [2, 3]. Figure 1.1 shows its essential elements. A probe tip, usually made of W or Pt–Ir alloy, is attached to a *piezodrive,* which consists of three mutually perpendicular piezoelectric transducers: x piezo, y piezo, and z piezo. Upon applying a voltage, a piezoelectric transducer expands or contracts. By applying a sawtooth voltage on the x piezo and a voltage ramp on the y piezo, the tip scans on the xy plane. Using the coarse positioner and the z piezo, the tip and the sample are brought to within a fraction of a nanometer each other. The electron wavefunctions in the tip overlap electron wavefunctions in the sample surface. A finite *tunneling conductance* is generated. By applying a bias voltage between the tip and the sample, a *tunneling current* is generated. The concept of tunneling will be presented in Section 1.2.

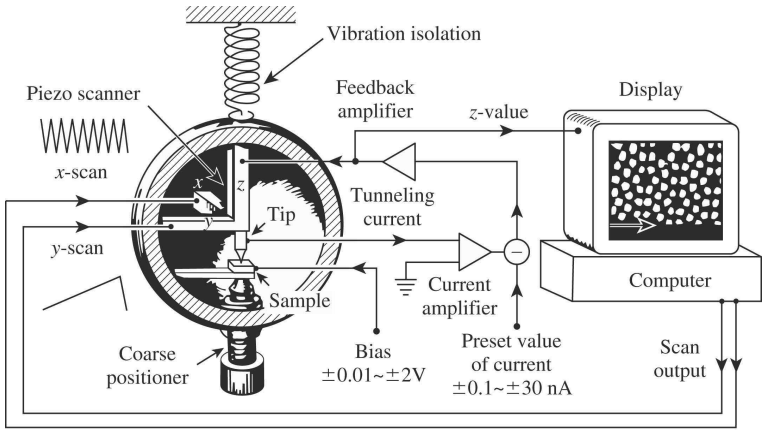

Fig. 1.1. The scanning tunneling microscope in a nutshell. The scanning waveforms, applying on the x and y piezos, make the tip raster scan on the sample surface. A bias voltage is applied between the sample and the tip to induce a tunneling current. The z piezo is controlled by a feedback system to maintain the tunneling current constant. The voltage on the z piezo represents the local height of the topography. To ensure stable operation, vibration isolation is essential.

The most widely used convention of the polarity of bias voltage is that the tip is virtually grounded. The bias voltage V is the *sample voltage*. If $V > 0$, the electrons are tunneling from the occupied states of the tip into the empty states of the sample. If $V < 0$, the electrons are tunneling from the occupied states of the sample into the empty states of the tip.

The tunneling current is converted to a voltage by the current amplifier, which is then compared with a reference value. The difference is amplified to drive the z piezo. The phase of the amplifier is chosen to provide a negative feedback: if the absolute value of the tunneling current is larger than the reference value, then the voltage applied to the z piezo tends to withdraw the tip from the sample surface, and *vice versa*. Therefore, an equilibrium z position is established. As the tip scans over the xy plane, a two-dimensional array of equilibrium z positions, representing a contour plot of the equal tunneling-current surface, is obtained, displayed, and stored in the computer memory.

The topography of the surface is displayed on a computer screen, typically as a gray-scale image, see Fig. 1.2(a). The gray-scale image is similar to a black-and-white television picture. Usually, the bright spots represent high z values (protrusions), and the dark spots represent low z values (depressions). The z values corresponding to the gray levels are indicated by a scale bar. For a more quantitative representation of the topography, a contour plot along a given line is often provided, as shown in Fig. 1.2(b). The most convenient unit for x and y is nanometer (nm, 10^{-9} m), and the most convenient unit for z is picometer (pm, 10^{-12} m).

To achieve atomic resolution, vibration isolation is essential. This is achieved by making the STM unit as rigid as possible, and by reducing the influence of environmental vibration to the STM unit. See Chapter 10.

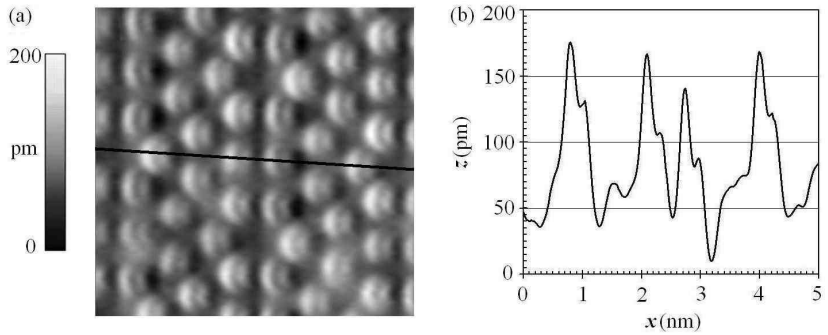

Fig. 1.2. Gray-scale image and contour plot. (a) A 5nm×5nm gray-level topographic image of Si(111)7×7. The bright spots represent protrusions, and the dark spots represent depressions. The z values corresponding to the gray levels are indicated by a scale bar. (b) The topographic contour along a line in (a), for a more quantitative representation. By courtesy of F. Giessibl.

1.5 Illustrative applications

Over the last decades, the applications of STM and AFM have grown so fast and so vast that a thorough review would take many volumes. And there are already many good books as well as review articles published on applications of STM and AFM in various fields. In this section, a few examples are presented as illustrations.

1.5.1 Catalysis research

Catalysis is the backbone of synthetic chemistry. It is a basic process in the production of fabrics, fuels, fertilizers and pharmaceuticals. Catalysis is also essential in environmental protection. For example, required by law, each automobile must have a *catalytic converter* to remove toxic exhaust gases, notably CO and NO_x. Although it is well known that catalytic reactions often take place at specific active atomic sites on the catalyst surface, the research in catalysis have been mainly relying on test-and-error experimentation involving macroscopic parameters. The invention of STM enables detailed studies of the electronic structures of the active sites at catalyst surfaces. STM can even operate in an atmosphere with actual reactants, thus to observe the transformation of molecules at active atomic sites on real time. Therefore, STM research can help facilitate a full understanding and control of the constituents at the molecular and atomic levels, and to open up the possibility of *designing the catalysis process at the single molecule level* [14]. Here are two examples.

Ni-Au catalyst for steam reforming

Steam reforming is a method in the chemical industry to produce hydrogen from hydrocarbons. For example, in the presence of a catalyst, alkanes react with steam (overheated water vapor) to generate H_2 and CO:

$$C_nH_{2n+2} + nH_2O \rightarrow n\,CO + (2n+1)\,H_2. \tag{1.1}$$

The most important case is the reaction of methane with steam,

$$CH_4 + H_2O \rightarrow CO + 3\,H_2. \tag{1.2}$$

It is the most common and least expensive method to produce hydrogen. The typical catalyst is nickel nanoclusters supported on a $MgAl_2O_4$ substrate. Nevertheless, in parallel with the steam reforming process, nickel also catalyzes the production of graphite, which impedes the activity due to the formation of a blocking carbon layer on the nickel surface (coking) and may eventually lead to the breakdown of the catalyst. An existing solution to that problem is by mixing a minute amount of H_2S to the reactants, which poisons the nickel catalyst. Because sulfur poisons the formation of

graphite more than it poisons the steam formation reaction, the lifetime of the catalyst is prolonged. However, the overall rate is lower, and the inclusion of H_2S is harmful to the subsequent processes and the environment.

A new idea comes from the STM studies of the Ni-Au system [15]. Ni and Au are immiscible in the bulk. No binary alloy can be formed. However, STM studies showed that by mixing a few percents of Au to Ni, after annealing at 800 K, a surface binary alloy is formed: many Ni atoms on the surface are substituted by Au atoms, see Fig. 1.3. The topographic STM image shows that as if the Au atoms are darker (deeper), and the Ni atoms immediately adjacent to an Au atom are brighter (higher). It is not because the Au atoms are depressed and the adjacent Ni atoms are protruded, but is an electronic effect inherent to STM. According to the Tersoff-Hamann model of STM imaging [16, 17] (see Chapter 6), a topographic STM image is the contour of equal Fermi-level local density of states of the sample, measured at the center-of-curvature of the tip $\mathbf{r_0}$, $\rho(E_F, \mathbf{r_0})$. On the Au atoms, the value of $\rho(E_F, \mathbf{r})$ is lower than that of the normal Ni atoms. On the other hand, the value of $\rho(E_F, \mathbf{r})$ of a Ni atom adjacent to a Au atom is higher owing to the perturbation by the Au atom. For a Ni atom with two Au neighbors, the perturbation is even stronger, see Fig. 1.3. Because the Fermi-level local density of states is closely related to catalytic reactivity, those Ni atoms provide a higher reactivity than the normal Ni atoms. Furthermore, the carbon atoms are much less likely to adsorb on the Ni atoms adjacent to a Au atom. The results are: by mixing a few percents of Au to Ni, the reactivity of the steam formation process is enhanced, and

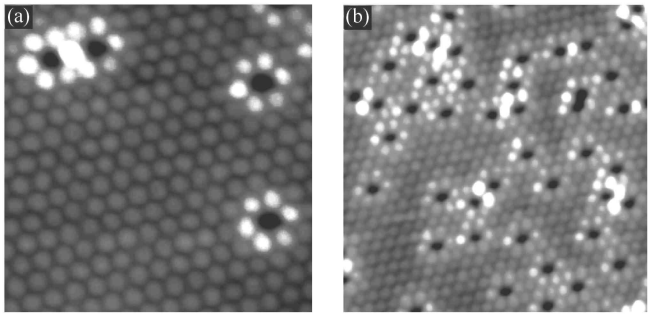

Fig. 1.3. STM topographical images of the Ni-Au system. (a) An image of Ni(111) with 2% Au. The Au atom appears as depressions because of the LDOS at the Fermi level is lower. The Ni atoms surrounding an Au atom appear as protrusions because of the enhancement of LDOS at the Fermi level, indicating a higher chemical reactivity. For the Ni atom between two Au atoms, the LDOS enhancement is even higher. (b) An image of Ni(111) surface with 7% of Au. The number of Ni atoms with doubly enhanced Fermi-level LDOS is increased. (Original figure in black-and-white with high resolution by courtesy of F. Besenbacher and J. V. Lauritsen. Reproduced with permission [15]. Copyright 1998 the American Association for the Advancement of Science.)

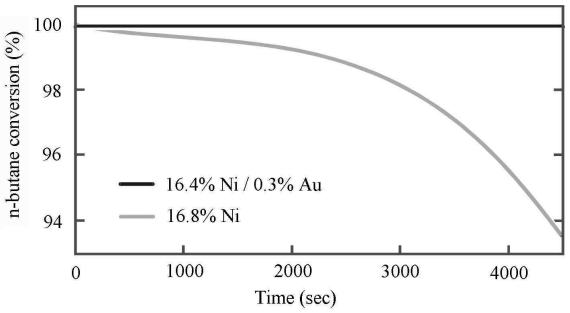

Fig. 1.4. Conversion rates of the Ni catalyst and the Ni-Au catalyst. The conversion rates of steam reformation of n-butane and water vapor using different catalysts. Gray curve: pure Ni catalyst. the rate deteriorates with time as a result of the parasitic graphite formation process. Black curve: Ni-Au catalyst, which shows no deterioration of reaction rate. (Original figure in black-and-white with high resolution by courtesy of F. Besenbacher and J. V. Lauritsen. Reproduced with permission [15]. Copyright 1998 the American Association for the Advancement of Science.)

the graphite formation process is reduced. While the conversion rate of the pure Ni catalyst decreases markedly after an hour of operation, the conversion rate of Ni-Au catalyst remains constant. Therefore, the Ni-Au catalyst could be active for a much longer time, see Fig. 1.4.

Based on the STM study, a new catalyst, with about 16.5 weight percents of Ni and 0.3 weight percents of Au on a $MgAl_2O_4$ matrix, is designed, which substantially improves the steam formation process.

Understand and improve the MoS_2 catalyst

Petroleum contains a wide range of sulfur compounds, for example, alkanethiol ($C_nH_{2n+1}SH$) and thiophene (C_4H_4S). Sulfur is harmful for the chemical processings and for the environment. The process to remove sulfur, *hydrodesulphurization* (HDS), is an essential step in petrochemical industry. The typical catalyst is molybdenum disulfate (MoS_2). In the presence of hydrogen, the HDS reaction converts alkanethiol into alkane,

$$C_nH_{2n+1}SH + H_2 \rightarrow C_nH_{2n+2} + H_2S, \tag{1.3}$$

and the gas-phase H_2S is easily removed.

MoS_2 is a layered material, similar to graphite. The bulk of MoS_2 consists of thin sheets of S-Mo-S sandwiches, and those sheets are held together by van der Waals forces. The basal planes of MoS_2 are chemically inert. Therefore, catalytic reactivity must reside in the rims of the sheets. However, before the application of STM, the preferred structure and the active sites of MoS_2 crystallites, as well as the reaction paths of the HDS process, were only vaguely guessed based on macroscopic evidences.

A systematic study of the structure, active sites, and reaction paths is carried out with STM experiments and DFT computations [18]. In the industry, $MgAl_2O_4$ is usually used as substrates for the MoS_2 clusters. However, it is not appropriate for STM studies because it is an insulator. For STM studies, single crystal gold is chosen as the substrate, especilly the Au(111) surface. Gold is relatively inert and allows for investigation of the intrinsic properties of the catalysts.

The nanoclusters of MoS_2 were prepared by depositing molybdenum on Au(111) surface in an atmosphere of H_2S at a pressure of 1×10^{-6} mbar, then the substrate was annealed to 673–723K for 15 minutes. A fairly uniform distribution of crystalline MoS_2 nanoclusters was formed. Most of the MoS_2 nanoclusters appear to have a triangular shape, with an average area of 5 nm^2. The side length of each triangular nanocluster is about 3 nm. From a combination of STM experiments and first-principles computations, it was concluded that the edges are saturated with sulfur atoms [18].

By exposing the MoS_2 nanoclusters with various substances, the reactivity of MoS_2 is studied with STM. It was found that MoS_2 neither reacts with organic molecules containing sulfur, such as alkanethiol ($C_nH_{2n+1}SH$)

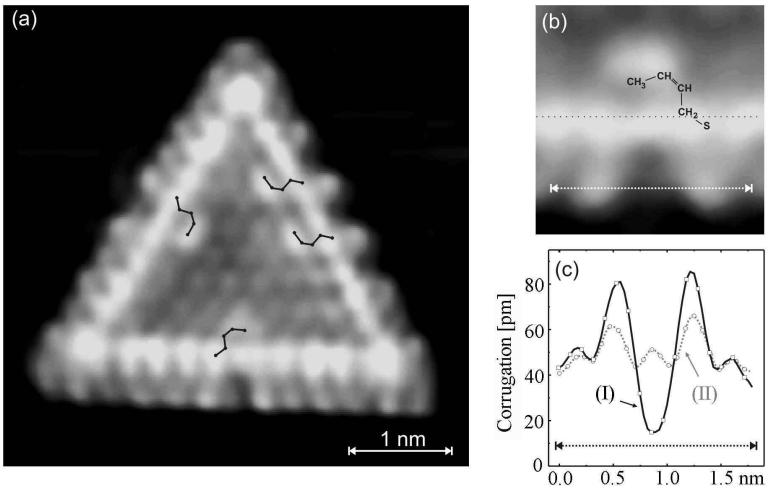

Fig. 1.5. Reaction of H and thiophene with a MoS_2 nanocluster. (a) The triangular MoS_2 nanocluster, after exposed to atomic hydrogen and then thiophene at elevated temperature, is cooled down and characterized by STM. Image size: 5×5 nm^2. Bean-like structures, identified as the intermediate product of thiophene, *cis*-but-2-ene-thiolate (CH_3-CH=CH-CH_2-S^-), are found on the bright rim. Also, there is a prominent change in the outermost rim protrusions, identified as sulfur vacancies. Part of the rim is highlighted in (b). Details of a line scan of the rim is shown in (c). Solid curve (I): STM line scan along the dashed line in (b). Dashed curve (II): the line scan of the correspondent unreacted area, shown for comparison. (Original high-resolution image in black-and-white by courtesy of J. V. Lauritsen. See [14, 18] for details.)

and thiophene (C_4H_4S), nor reacts with H_2. Only after exposing MoS_2 with predissociated (atomic) hydrogen, visible changes are observed. Sulfur vacancies are created at the rims.

By further exposing the MoS_2 nanoclusters already treated with atomic hydrogen with thiophene (C_4H_4S), a strong reaction is found, as shown in Fig. 1.5. As shown, parts of the rim are significantly altered. The outermost protrusions of the rims are markedly shifted, and bean-like structures appear adjacent to the bright rim.

The STM study revealed the mechanism of catalytic reaction. First, a hydrogen atom reacts with the rim of a MoS_2 nanocluster, strip off a sulfur atom and expose a molybdenum atom. The molybdenum atom becomes an active site. A alkanethiol molecule can chemically adsorb on the active site by forming a S-Mo bond. After picking up a H atom, the hydrocarbon molecule becomes free, and the sulfur atom occupies the S vacancy at the rim of the MoS_2 nanocluster. The desulphurization of thiophene is more complex. At an active site of MoS_2, it is first converted to an intermediate product, *cis*-but-2-ene-thiolate (CH_3-CH=CH-CH_2-S^-), and adsorbs on the bright rim. Then it reacts further with hydrogen to become H_2S and alkenes.

The detailed understanding of the catalytic reaction at the atomic level has resulted in improvements of the hydrodesulphurization catalyst.

1.5.2 Atomic-scale imaging at the liquid-solid interface

The atomic-scale phenomena at the liquid-solid interface is of significant scientific and technological interest. Electrochemistry, and the related chemical industry, is based on atomic-scale reactions at the liquid-solid interface. Most of the biological objects are only active in aqueous buffer solutions. However, the traditional method for characterizing the surface relies on ultra high vacuum, which cannot access the liquid-solid interface. The invention of STM and AFM opened a wide window to study the atomic-scale phenomena at the liquid-solid interface. Experiments showed that if the liquid is clean, atomic resolution can be readily achieved. Furthermore, the well-established methods of electrochemistry can be applied to change the surface and the adsorbed atoms and molecules.

The pioneering works in this field [19, 20] showed a great potential of operating STM in liquids by using a two-electrode system: the substrate and the STM tip. Later on, by combining STM with the standard methods of electrochemistry [21, 22], a four-electrode system was introduced [23, 24], which provides a powerful, general and convenient method to study the liquid-solid interface and a large number of electrochemical processes down to atomic level.

Figure 1.6 is a schematic of STM in an electrochemistry cell. The standard electrochemistry cell contains three electrodes [25]. The working electrode (WE) is the substrate under investigation. The reference electrode

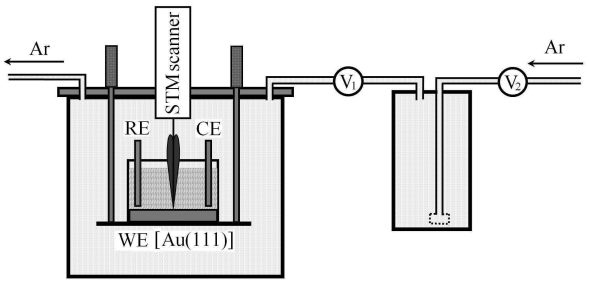

Fig. 1.6. The four-electrode electrochemical cell with STM. The standard electrochemical cell has three electrodes: the working electrode (WE), the reference electrode (RE), and the counter electrode (CE). By ramping the potential of the working electrode back and forth, a cyclic current-potential curve can be generated. The STM tip is the fourth electrode, to provide tunneling with the working electrode. To prevent the harmful effect of oxygen, the entire cell is placed in argon atmosphere. (Original figure by courtesy of J. Ulstrup's group of Technical University of Denmark. See [26] for details.)

(RE) provides the reference potential, with insignificant electrical current flow. Typically, a saturated calomel electrode (SCE) is used as the reference electrode [25]. The counter electrode (CE) supports the Faradaic current to or from the working electrode. A routine experiment in electrochemistry consists of a cycle to ramp the potential of the working electrode up and down with regard to the reference electrode. The Faradaic current is recorded as a function of time, thus also a function of potential. The cyclic current-potential curve, the so-called *cyclic voltammogram*, contains a rich body of information regarding the electrochemistry at the liquid-solid interface.

For STM experiments, a fourth electrode, the STM tip, is introduced. The tip should be covered with an insulating film except on the very end of the tip. The technique of making such a tip is described in Section 13.6.

Oxygen often reacts with the adsorbates of interest, especially biological molecules. To improve the cleanness of the liquid-solid interface, oxygen should be removed from the electrolyte. An effective method is to enclose the entire system in an inert-gas atmosphere, such as nitrogen or argon. To reduce the vibration caused by the flow of inert gas, a buffer bottle and two valves are installed to limit the flow rate, see Fig 1.6.

As in all STM-related experiments, an important issue is to start with an atomically flat, well-defined and well-understood substrate surface. The Au(111) surface is an excellent substrate for the operation of STM in liquid. Small pieces of single crystal gold can be generated by flame annealing using a H_2 flame. The single crystal, typically a few mm in diameter, shows different crystallographic planes on its surface. After identified, a small piece of gold chip is cut off from the sphere then mounted on a sample holder. Au(111) samples can also be made by vacuum depositing gold on mica,

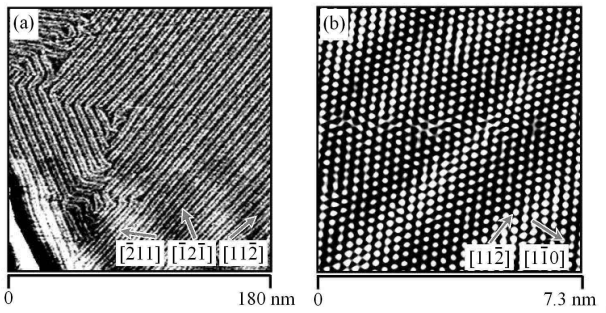

Fig. 1.7. Au(111) surface imaged by STM in liquids. (a) At relatively large scale, the $22\times\sqrt{3}$ reconstruction should be observed readily. (b) At smaller scale, individual atoms should be observed. It provides a calibration of the x, y scales. (Original images by courtesy of J. Ulstrup's group of Technical University of Denmark.)

followed by annealing. The advantage of gold is that it does not oxidize in air, thus the samples can be transferred through air. If the STM system works properly, the $22\times\sqrt{3}$ reconstruction should be observed readily, see Fig. 1.7(a). This provides a natural calibration for the x, y scales, and the identification of the crystallographic orientations of the gold surface with regard to the scan directions. If the tip is in good condition, atomic resolution is achievable, see Fig. 1.7(b).

In the UHV environment, in order to change the surface reconstruction, depositing or removing a layer of atoms or molecules at the surface, time-consuming and often irreversible annealing and vacuum evaporation processes are required. In an electrochemical cell, those processes could be accomplished within seconds by simply changing the potential, and are almost always reversible. For example, the *potential-induced reconstruction* has been observed on all three low-Miller-index gold surfaces. In 0.1M H_2SO_4, for potential U_s <0.73 V, there is no stable SO_4^{2-} adlayer. For potential U_s >0.73 V, a full ordered adlayer of SO_4^{2-} is formed. Figure 1.8(a) shows a voltammogram of the Au surface in 0.1M H_2SO_4. The first peak at about 0.35 V corresponds to the transition from the $22\times\sqrt{3}$ reconstruction to the Au(111)-1×1 structure. The second peak around 0.73 V corresponds to the formation of an ordered adlayer of sulfate. The very narrow peak means that the ordered adlayer is formed within a very small potential range. Figure 1.8(b) is an STM image of the Au(111) surface, recorded at different potentials. The upper half, recorded at a potential of 0.65 V, shows atomic resolution of the Au(111)-1×1 surface. The lower half, recorded at a potential of 0.8 V, shows an ordered adlayer of sulfate.

In order to observe large biomolecules such as nucleotides and proteins with STM or AFM in aqueous solutions, a key step is *immobilization*: to adsorb the molecule on a flat surface without changing its functions. A

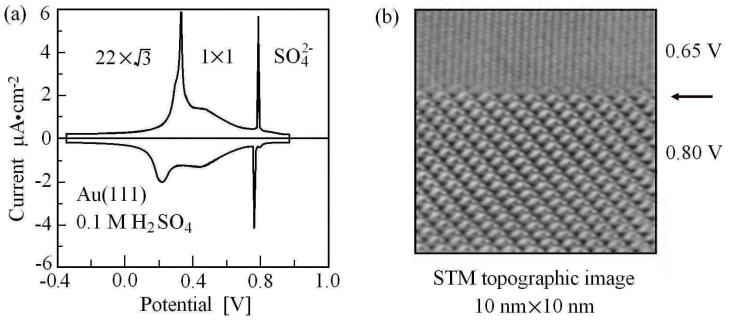

Fig. 1.8. A voltammogram and an STM image of Au in 0.1M H_2SO_4. (a) A voltammogram of Au in 0.1M H_2SO_4. It starts at -0.35 V with a freshly prepared Au(111)-22×$\sqrt{3}$ reconstruction. The broad peak at 0.35 V signals the transition from the Au(111)-22×$\sqrt{3}$ reconstruction to a 1×1 structure. The very sharp peak at around 0.73 V corresponds to the formation of an ordered adlayer of sulfate. (b) An STM image of the Au(111) surface, taken at 0.65 V first, then changed the potential to 0.8 V. An order adlayer of sulfate is formed. (Adapted with permission from Kolb [24]. Copyright Wiley-VCH Verlag GmbH & Co. KGaA.)

commonly used method is to start with self-assembled monolayers of thiols on atomically flat gold surfaces, for example, Au(111). The thiols, the organic molecules with a thiol functional group -SH, can form a strong S-Au bond on gold surfaces (about 1 eV), leading to self-assembled monolayers. The other functional groups in that molecule, such as -OH, -CH_3, -CHO, could provide immobilizing anchors to the molecules of interest. Alkanethiols $C_nH_{2n+1}SH$ are the most commonly used thiols to form self-assembled monolayers. Organic molecules containing carboxyl (-COOH) and amine (-NH_2) functional groups are important for immobilization of biological macromolecules. Among the thiols, cysteine is of particular interest [27].

Cysteine (HS-CH_2-$CHNH_2$-COOH) is one of the 20 amino acids in proteins, an indispensable building block of biological systems. Cysteine is a particularly important building block in the formation of human hair, fingernails, skin, and wool, and a ligand in many metalloproteins. Cysteine is one of the two amino acids which contain sulfur, and the only amino acid which contains a thiol group. A self-assembled monolayer of cysteine on gold surface provides both the carboxyl group and the amine group for the immobilization of biological macromolecules, especially proteins.

Self-assembled monolayers of cysteine are formed by exposing Au(111) to a dilute solution of cysteine in 50 mM aqueous buffer electrolyte of ammonium acetate (CH_3COONH_4) [27]. The advantage of using ammonium acetate is that pH is around 4.6, is mild to biomolecules, and it does not adsorb on Au(111) surface over a quite wide potential range. A cysteine concentration of 1×10^{-6} M is sufficient to build a highly ordered cysteine monolayer under potential control. A gradual disappearance of the herring-

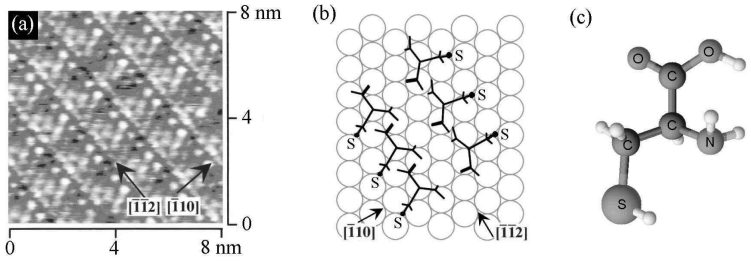

Fig. 1.9. Self-assembled monolayer of cysteine on Au(111). (a) A STM image of the self-assembled monolayer of cysteine on Au(111). (b) Proposed model of its structure. The sulfur atom is bonded to the Au(111) surface at the hollow site. (c) A ball-and-stick model of cysteine. (Original figure by courtesy of J. Ulstrup's group of Technical University of Denmark. Reproduced with permission [27]. Copyright 2000 American Chemical Society.)

bone pattern of the STM image signifies its formation.

A typical STM image of a highly ordered monolayer of cysteine thus obtained is shown in Fig. 1.9(a). A structural model derived from the experiments is shown in Fig. 1.9(b). A ball-and-stick model of cysteine is shown in Fig. 1.9(c). As shown, the sulfur atom is bonded to a hollow site of the Au(111) surface. The lateral interactions of cysteine finally generates an ordered pattern.

1.5.3 Atom manipulation

In the speech entitled *There's Plenty of Room at the Bottom: An Invitation to Enter a New Field of Physics* [1], Richard Feynman posed a question "Why cannot we write the entire 24 volumes of the Encyclopedia Britannica on the head of a pin?" Such a dense writing requires that each dot of the letters is 8 nm in diameter, a length of about 32 atoms in an ordinary metal. In other words, each dot would contain in its area about 1,000 atoms. At that time, such a dense writing was a fantasy.

The invention of STM has completely changed the scenario. Using STM as a writing tool, features made of single atoms can be generated, far exceeded the goal of Feynman. With such a density, the publications of the entire US Congress Library could be written on the head of a pin.

The basic operation of atom manipulation is to use the STM tip to move an adatom from an initial position to a new position on a substrate, as shown in Fig. 1.10. At the beginning, the atom for the designed structure is deposited randomly on a substrate. Each atom is then an adatom on the substrate at a random position. In order to move an adatom to another stable location, an activation energy E must be applied to lift it across a ridge to reach another stable position.

There are three steps for a move, see Fig. 1.10. Step A is to place the

tip at the top of an adatom to be moved, then gradually increase the set tunneling current. As a result, the tip moves towards the adatom. A partial chemical bond is formed. When the chemical bond energy equals the barrier energy, the tip should be able to pull the adatom over the ridge. Step B is to move the tip sideways to pull the adatom to a desired location. Step C is to gradually decrease the set tunneling current. As a result, the tip moves away from the adatom and leaves it at the new position.

During the process of atom manipulation, neither the interaction energy between the tip and the adatom nor the distance between the apex atom of the tip and the adatom is known. The pioneers of atom manipulation found from experience that this can be controlled by tunneling conductance, or its inverse, the tunneling resistance. The threshold interaction energy to allow the tip to pull the adatom over a diffusion barrier corresponds to a *threshold conductance*, or equivalently, a *threshold resistance* [28, 29]. There is a general and fundamental relation between interaction energy and tunneling conductance, which will be discussed in Chapter 5.

An example of the writing process is shown in Fig. 1.11. Those Chinese characters were written using Ag atoms on Ag(111) surface using the above process. At each stage of the manipulation, an image could be taken to show the progress and to figure out the next steps to be executed. The area of a complete Chinese character is 12 nm×12 nm. The size of each dot is less than 0.8 nm×0.8 nm, 100 times smaller than that proposed by Feynman.

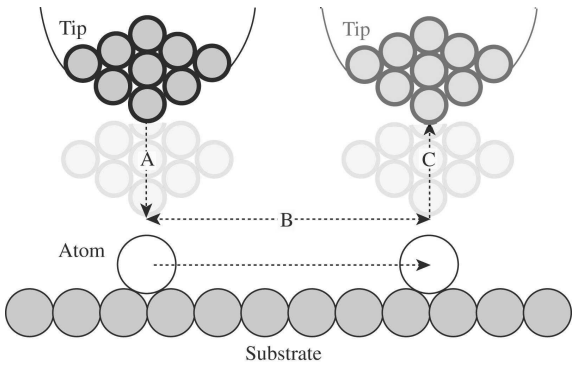

Fig. 1.10. The basic steps of atom manipulation. First, position the tip to above the adatom to be moved. Then, following the three steps: Step A, gradually increase the set tunneling current to move the tip towards the adatom, until the interaction energy between the tip and the adatom reaches the *diffusion activation energy*, the energy required to move the adatom across the ridge between two adjacent stable positions. Step B, pull the adatom to a desired location. Step C, gradually decrease the set tunneling current to move the tip away from the adatom.

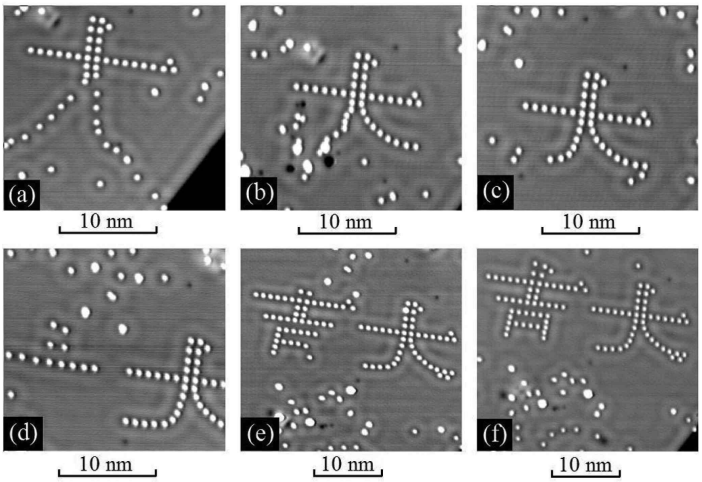

Fig. 1.11. Writing Chinese characters using STM. A sequence of STM images showing the assembly of two Chinese characters from single Ag atoms on a Ag(111) surface. The lateral manipulation technique allows the exact placing of single atoms on desired atomic sites. An assembly involves not only the movement of single atoms but requires also many repair and cleaning steps until the final structure is completed [1]. (Courtesy of K.-F. Braun and N. Pertaya, Freie Universität Berlin.)

1.5.4 Imaging and manipulating DNA using AFM

In the same speech, *There's Plenty of Room at the Bottom* [1], Richard Feynman also proposed an approach for biology research using a microscope capable of resolving individual atoms.

> What are the most central and fundamental problems of biology today? They are questions like: What is the sequence of bases in the DNA (*deoxyribonucleic acid*)? What happens when you have a mutation? How is the base order in the DNA connected to the order of amino acids in the protein?...
>
> It is very easy to answer many of these fundamental biological questions; you just look at the thing! You will see the order of bases in the chain; you will see the structure of the microsome. Unfortunately, the present microscope sees at a scale which is just a bit too crude. Make the microscope one hundred times more powerful, and many problems of biology would be made very much easier.

The invention of STM and AFM brings Feynman's ultimate goal a lot closer. Since the resolution of optical microscopy is limited by the wavelength of light, which is a fraction of a micrometer, nearly atomic resolution

is in principle impossible. The scanning electron microscope and the transmission electron microscope can achieve a much better resolution. However, the samples must be placed in a vacuum chamber, and often coated with metal or other substances. At best those methods resemble a kind of autopsy. STM and AFM can, in principle, image *live* biological molecules, and it is possible to image the *process*.

Because the biological molecules are poor conductors, AFM is more suitable. The AFM experiments are often performed in air or in an aqueous buffer solution at room temperature. As long as proper sterilization is carried out, clean environment could be achieved. Since the static-mode AFM often damages the sample, tapping mode is frequently used. Commercial AFM, such as Nanoscope IIIa, with commercial cantilevers and tips, can be conveniently utilized. To date, true atomic resolution on biological molecules is rarely achieved. Nevertheless, the nanometer-scale resolution has already provided a lot of unprecedented first-hand microscopic information on biological molecules. See Chapter 15 for details.

Immobilization and imaging

In order to use AFM to take images, the biological molecules must be immobilized on an atomically flat surface without impairing its biological activity. In Section 1.5.2, the method of immobilization for STM in an electrochemical environment is discussed. Gold surface with a self-assembled monolayer of thiol derivatives is presented. For AFM, an insulating substrate works equally well. One of the best substrates is *silanated mica* [30].

Mica can be easily cleaved to create atomically flat surfaces. However, biomolecules do not adsorb on native mica surfaces. Treating mica with a silanation agent, for example, 3-aminopropyl triethoxysilane (NH_3-$(CH_2)_3$-Si-$(O$-$C_2H_5)_3$, usually abbreviated as APTS), dramatically improves adhesion. Here, an ethyl group (-C_2H_5) of APTS reacts with a hydroxyl group (-OH) of mica, and then a strong Si-O-Si bond is formed. The amine group (-NH_2) is exposed and enables the adsorption of biomolecules.

Nevertheless, the bonding of DNA on APTS-treated mica is a little too strong, thus the DNA molecules are often entangled. This situation can be corrected using the method of "molecule combing": by forcing a fluid flow parallel to the surface, the DNA molecules are aligned to the direction of the flow, thus effectively disentangled [31]. The original method was demonstrated on glass surfaces. However, glass surface is not flat enough for nanometer-scale AFM studies. By applying the molecule-combing method to mica, under well-controlled conditions, very straight, parallel DNA strands can be generated, as verified by AFM images [30].

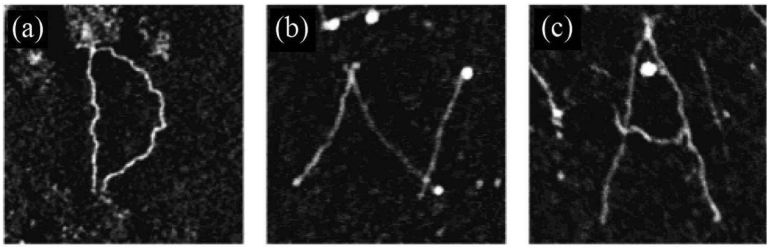

Fig. 1.12. Manipulating DNA molecules using AFM. A pattern of DNA molecules fabricated by AFM. First, DNA strands are deposited on an AP-mica surface. Second, the AFM tip is positioned to a predefined location of the DNA strand, then pressed hard to cut it. Third, the AFM tip is used to sweep or push the DNA strands to form a designed pattern. (Reproduced from [32], with permission.)

DNA manipulation

The AFM has achieved beyond the target of Feynman: it is capable of not only *imaging*, but also *manipulating* the biological molecules. Figure 1.12 shows an example of imaging *and* manipulating DNA molecules [32].

In those experiments, the DNA molecules are deposited on a mica surface, pretreated with APTS for good adhesion. Those DNA strands are first processed with a flowing buffer fluid, to form a more-or-less regular pattern. Then, the AFM tip is used to manipulate the DNA strands to fabricate designed patterns by the following sequence of actions.

The first action is *molecular cutting*. By positioning the tip at a predetermined location of the DNA strand, then pressing it hard, the DNA strand could be broken at a point of nanometer accuracy.

The second action is sweeping or pushing. A fragment of a DNA strand could be pushed by the side of the AFM tip, either to move it out of the area of interest, or to reposition it to a predetermined location.

During the entire process, the DNA strands can be imaged with tapping mode using the same AFM tip at any time. In Fig. 1.12, the DNA strands are cut and pushed to create three letters: DNA.

DNA surgery

By combining the capability of AFM to manipulate the DNA with the established methods in molecular biology, a procedure of *DNA surgery* was demonstrated [33, 34]. Besides imaging, the AFM tip can dissect a DNA molecule at designated positions, and then pick up a desired segment. The tip, which holds the DNA segment, is transferred into a test tube. Using the *polymerase chain reaction* process (PCR), invented by Kary Mullit [35], the single DNA segment can be multiplied into billions of copies within a few hours in a test tube with the help of an enzyme *polymerase*. For a rerview of PCR, see Chapter 8 of [36]. The order of the nucleotide bases of the large

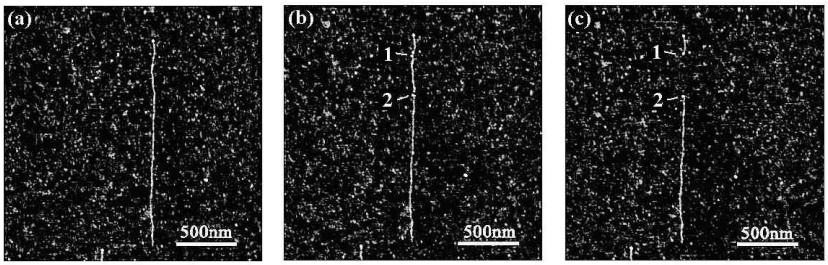

Fig. 1.13. Cutting and picking up a DNA segment using AFM. (a) The original DNA fragment. (b) The DNA fragment was cut at 150 nm and 450 nm locations. (c) The DNA segment was missing in the subsequent images, after picked up by the AFM tip. (Reproduced with permission from [34]. Copyright 2007 Institute of Physics.)

number of identical DNAs can be sequenced by the Sanger method. For a review of the Sanger sequencing method, see Chapter 12 of [36].

The proof-of-concept experiment was performed with a relatively small and well-understood DNA molecule, the linearized pRB322. It has 4362 base pairs (bp) and a theoretical length of 1483 nm. The experiment was performed using Nanoscope IIIa in air at room temperature. The pBR322 DNA molecules were deposited on a APTS-pretreated mica substrate, then straightened using the molecule-combing method.

Figure 1.13(a) shows an AFM image of the as deposited DNA molecule. The DNA molecule was then dissected at two predetermined points to create an isolated segment, see Fig. 1.13(b). By pushing the side of the tip against that segment, it could adhere onto the tip. By imaging the substrate again with AFM, it appeared the segment was missing, see Fig. 1.3(c).

To verify that the DNA segment was actually picked up by the AFM tip, the tip was transferred into a sterile tube for a PCR process [35, 36]. The results of PCR were then investigated by Sanger sequencing. In the very first set of experiments, among 20 attempts, 7 cases were positive: the expected DNA segments were detected [33, 34].

Bibliography

[1] R. P. Feynman. *There's Plenty of Room at the Bottom: An Invitation to Enter a New Field of Physics*. Lecture at an 1959 APS meeting. The Archives, California Institute of Technology, see www.its.caltech.edu/∼feynman/plenty.html (1959).

[2] G. Binnig, H. Rohrer, Ch. Gerber, and E. Weibel. Tunneling through a controllable vacuum gap. *Appl. Phys. Lett.* **40**, 178–180 (1982).

[3] G. Binnig, H. Rohrer, Ch. Gerber, and E. Weibel. Surface studies by scanning tunneling microscopy. *Phys. Rev. Lett.* **49**, 57–61 (1982).

[4] G. Binnig, C. F. Quate, and Ch. Gerber. Atomic force microscope. *Phys. Rev. Lett.* **56**, 930–933 (1986).

[5] G. Binnig and H. Rohrer. Scanning tunneling microscopy – from birth to adolescence. *Rev. Mod. Phys.* **59**, 615–625 (1987).

[6] G. Binnig and H. Rohrer. In touch with atoms. *Rev. Mod. Phys.* **71**, S324–S330 (1999).

[7] C. J. Chen. *Introduction to Scanning Tunneling Microscopy*. First Edition, Oxford University Press, New York (1993).

[8] R. Buderi. *Engines of Tomorrow: How the World's Best Companies Are Using their Research Labs to Win the Future*. Simon and Schuster, New York (2000). See pages 150 and 151.

[9] R. Wiesendanger. *Scanning Probe Microscopy and Spectroscopy: Methods and Applications*. Cambridge University Press (1994).

[10] Ed. R. Wiesendanger and H.-J. Güntherodt. *Scanning Tunneling Microscopy I, II, III*. Springer-Verlag (1993).

[11] Ed. J. A. Stroscio and W. J. Kaiser. *Scanning Tunneling Microscopy*. Academic Press (1993).

[12] C. Bai. *Scanning Tunneling Microscopy and its Applications*. Second, Revised Edition, Springer and Shanghai Scientific and Technical Publishers (1999).

[13] Ed. D. Bonnell. *Scanning Probe Microscopy and Spectroscopy: Theory, Techniques, and Applications*. Second Edition, Wiley-VCH (2000).

[14] J. V. Lauritsen and F. Besenbacher. Model catalyst surfaces investigated by scanning tunneling microscopy. *Adv. Catal.* **50**, 97–147 (2006).

[15] F. Besenbacher, I. Chorkendorff, B. S. Clausen, B. Hammer, J. K. Norskov, and I. Stensgaard. Design of a surface alloy catalyst for steam reforming. *Science* **279**, 1913–1915 (1998).

[16] J. Tersoff and D. R. Hamann. Theory and application for the scanning tunneling microscope. *Phys. Rev. Lett.* **50**, 1998–2001 (1983).

[17] J. Tersoff and D. R. Hamann. Theory of scanning tunneling microscope. *Phys. Rev. B* **31**, 805–814 (1985).

[18] J. V. Lauritsen, M. Nyberg, R. T. Vang, M. V. Bollinger, B. S. Clausen, H. Topsoe, K. W. Jacobsen, E. Laegsggard, J. K. Norskov, and F. Besenbacher. Chmistry of one-dimensional metallic edga states in MoS_2 nanoclusters. *Nanotechnology* **14**, 385–389 (2003).

[19] R. Sonnenfeld and P. K. Hansma. Atomic-resolution microscopy in water. *Science* **232**, 211–213 (1986).

[20] R. Sonnenfeld, J. Schneir, and P. K. Hansma. Scanning tunneling microscopy: A natural for electrochemistry. *Modern Aspects of Electrochemistry,* **21**, 1–28 (1990).

[21] K. Itaya and E. Tomita. Scanning tunneling microscopy for electrochemistry – a new concept for the in situ scanning tunneling microscopy in electrolyte solutions. *Surface Science Letters* **201**, L507–L512 (1988).

[22] J. Wiechers, T. Twomey, and D. M. Kolb. Electrochemical surface science. *J. Electroanal. Chem.* **248**, 451–460 (1988).

[23] K. Itaya. Scanning tunneling microscopy for electrochemistry – a new concept for the in situ scanning tunneling microscopy in electrolyte solutions. *Progress in Surface Science* **59**, 121–248 (1998).

[24] D. M. Kolb. Electrochemical surface science. *Angew. Chem. Int. Ed.* **40**, 1162–1181 (2001).

[25] A. J. Bard and L. R. Faulkner. *Electrochemical Methods: Fundamentals and Applications, 2nd Edition*. John Wiley and Sons (2001).

[26] J. Zhang and J. Ulstrup. Oxygen-free in-situ scanning tunneling microscopy. *J. Electroanal. Chem.* **599**, 213–220 (2007).

[27] J. Zhang, Q. Chi, J. U. Nielsen, E. P. Friis, J. E. T. Andersen, and J. Ulstrup. Two-dimensional cysteine and cystine cluster networks on Au(111) disclosed by voltammetry and in-situ scanning tunneling microscopy. *Langmuir* **16**, 7229–7237 (2000).

[28] J. A. Stroscio and D. M. Eigler. Atomic and molecular manipulation with the scanning tunneling microscope. *Science* **254**, 1319–1326 (1991).

[29] P. Zeppenfeld, C. P. Lutz, and D. M. Eigler. Manipulating atoms and molecules with a scanning tunneling microscope. *Ultramicroscopy* **42–44**, 128–133 (1992).

[30] J. Hu, M. Wang, H.-U. G. Weier, P. Frantz, W. Kolbe, D. F. Ogletree, and M. Salmeron. Imaging of single extended DNA molecules on flat APS-mica by atomic force microscopy. *Langmuir* **12**, 1697–1700 (1996).

[31] A. Bensimon, A. Simon, A. Chiffaudel, V. Croquette, F. Heslot, and D. Bensimon. Aignment and sensitive detection of DNA by a moving interface. *Science* **265**, 2096–2098 (1994).

[32] J. Hu, Y. Zhang, H. Gao, M. Li, and U. Hartmann. Artificial DNA patterns by mechanical nanomanipulation. *Nano Letters* **2**, 55–57 (2002).

[33] J. H. Lü, H. K. Li, H. J. An, G. H. Wang, Y. Wang, M. Q. Li, Y. Zhang, and J. Hu. Positioning isolation and biochemical analysis of single DNA molecules based on nanomanipulation and single-molecule PCR. *J. Am. Chem. Soc* **126**, 11136–11137 (2004).

[34] H. J. An, J. H. Huang, M. Lü, X. L. Li, , J. H. Lü, H. K. Li, Y. Zhang, M. Q. Li, and J. Hu. Singe-base resolution and long-coverage sequencing based on single-molecule nanomanipulation. *Nanotechnology* **18**, 225101 (2007).

[35] K. B. Mullis. The unusual origin of the polymerase chain reaction. *Scientific American* **262**, 56–62 (1990).

[36] J. Sambrook and D. Russel. *Molecular Cloning: A Laboratory Manual*. 3rd edition, Cold Spring Harbor Laboratory Press, New York (2001).